Quantum Hyperdiffusion in One-Dimensional Tight-Binding Lattices

Zhenjun Zhang,[1] Peiqing Tong,[1,*] Jiangbin Gong,[2,3] and Baowen Li[2,3,4]

[1]*Department of Physics and Institute of Theoretical Physics, Nanjing Normal University, Nanjing, Jiangsu 210046, People's Republic of China*

[2]*Department of Physics and Centre for Computational Science and Engineering, National University of Singapore, Singapore 117542, Republic of Singapore*

[3]*NUS Graduate School for Integrative Sciences and Engineering, Singapore 117597, Republic of Singapore*

[4]*Centre for Phononics and Thermal Energy Science, Department of Physics, Tongji University, 200039, Shanghai, People's Republic of China*

(Received 26 August 2011; published 15 February 2012)

Transient quantum hyperdiffusion, namely, faster-than-ballistic wave packet spreading for a certain time scale, is found to be a typical feature in tight-binding lattices if a sublattice with on-site potential is embedded in a uniform lattice without on-site potential. The strength of the sublattice on-site potential, which can be periodic, disordered, or quasiperiodic, must be below certain threshold values for quantum hyperdiffusion to occur. This is explained by an energy band mismatch between the sublattice and the rest uniform lattice and by the structure of the underlying eigenstates. Cases with a quasiperiodic sublattice can yield remarkable hyperdiffusion exponents that are beyond three. A phenomenological explanation of hyperdiffusion exponents is also discussed.

DOI: 10.1103/PhysRevLett.108.070603 PACS numbers: 05.60.Gg, 03.65.−w, 71.23.−k, 72.20.Dp

In classical physics, the mean square displacement of a Brownian particle can be anomalous [1], i.e., $\langle \Delta x^2(t) \rangle \sim t^{\nu}$, with $\nu \neq 1$. Classical anomalous diffusion plays a vital role in complex systems [2] and is connected with many theoretical topics in statistical physics [3–6]. However, classical hyperdiffusion ($\nu > 2$), recently found for Brownian particles under the interplay of certain potentials and environments [7,8], is the least understood case with wide interest.

On the quantum side, wave packet spreading dynamics is unusually rich [9–16] in the absence of any environment. For particles in a one-dimensional (1D) tight-binding lattice, the mean square displacement is given by $\sigma^2(t) \equiv \Sigma_n n^2 |\psi_n(t)|^2 \sim t^{\gamma}$, where n is the lattice site index and $\psi_n(t)$ depicts a normalized time-evolving wave packet. Apart from ballistic diffusion ($\gamma = 2$) in uniform lattices [9] and localization ($\gamma = 0$) in disordered lattices [10], superdiffusion ($1 < \gamma < 2$) and subdiffusion ($0 < \gamma < 1$) can also occur in quasiperiodic lattices [12,15]. As to quantum hyperdiffusion ($\gamma > 2$ for a certain time scale), to our knowledge, it was first discovered in Ref. [16] but there is no further progress since then.

To gain more insight into quantum hyperdiffusion and to stimulate its experimental realizations using cold atoms in optical lattices [17], in this work we examine quantum wave packet dynamics in several nonuniform 1D tight-binding lattices, where a sublattice with on-site potential is embedded in a uniform lattice without on-site potential. Irrespective of whether the sublattice on-site potential is periodic, disordered (some disordered cases were studied in Ref. [16]), or quasiperiodic, we find threshold values of the on-site potential strength, beyond which quantum hyperdiffusion ceases to exist (in the disordered case, the observed disappearance of hyperdiffusion is based on a fixed number of realizations of the sublattice). This is explained via an energy band mismatch between the sublattice and the rest uniform lattice and via the structure of the underlying eigenstates. Such threshold values for observing quantum hyperdiffusion should be one key element in experimental studies. Furthermore, we predict from our numerical studies that the quantum hyperdiffusion exponent γ can be extensively tuned. Significantly, for quasiperiodic sublattices we observe quantum hyperdiffusion with $\gamma > 3$, by tuning the on-site potential strength or the length of the sublattice. As an extension of Ref. [16], a phenomenological explanation for quantum hyperdiffusion exponents is also discussed. The results should be within reach of today's cold-atom experiments.

Consider then the following 1D tight-binding time-dependent Schrödinger equation ($\hbar = 1$ throughout),

$$i\frac{\partial \psi_n(t)}{\partial t} = -\psi_{n+1}(t) - \psi_{n-1}(t) + V_n \psi_n(t), \qquad (1)$$

where V_n represents the dimensionless on-site potential scaled by a tunneling rate, for a sublattice of length $(2L + 1)$ with $n \in [-L, L]$. That is, $V_n \neq 0$ only when $n \in [-L, L]$. At time zero a localized wave packet is launched in the sublattice center, with $\psi_n(t = 0) = \delta_{n,0}$. Note that this initial state is a coherent superposition of many quasimomentum eigenstates. Some computational details are provided in our Supplemental Material [18].

Periodic case.—As a simple example of a periodic on-site potential, here we let $V_n = (-1)^n V$ ($V > 0$) for $L = 50$. The time dependence of $\sigma^2(t)$ is shown in

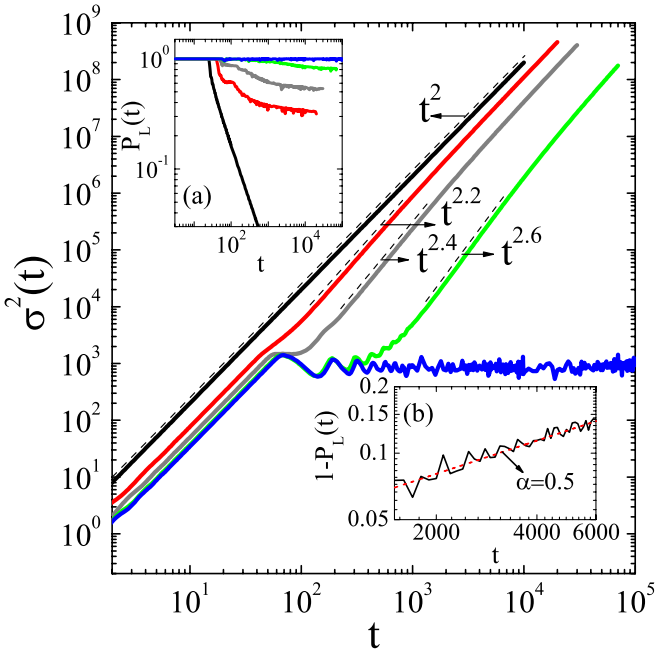

FIG. 1 (color online). Time dependence of $\sigma^2(t)$ for a periodic sublattice (with $L = 50$). From top to bottom, $V = 0$, 1, 1.5, 1.9, and 2. Here and in all other figures, dashed lines represent a power-law fitting and all plotted quantities are dimensionless. Inset (a) shows $P_L(t)$, with $V = 0$, 1, 1.5, 1.9, and 2 from bottom to top. In the case of $V = 1.9$ and for $1500 < t < 6000$, inset (b) shows (double-logarithmic scale) a nonlinear fitting of $P_L(t)$ using $P_L(t) = 1 - \Gamma t^{\alpha}$, with $\alpha = 0.5$.

Fig. 1, for increasing values of V. For all the shown cases the wave packet spreading is ballistic during the first stage of evolution. This is expected because the wave packet needs time to travel to the boundary between the sublattice and the rest. During the second stage, quantum hyperdiffusion is clearly observed except for $V = 0$ or for $V \geq V_c = 2$, with the diffusion exponent determined by power-law fitting represented by the dashed lines in Fig. 1. The time interval covered by these dashed lines also gives the actual duration of quantum hyperdiffusion, during which both t and $\sigma^2(t)$ can increase by about 1 order of magnitude. An increasing V is seen to enhance the diffusion exponent γ from $\gamma \approx 2.0$ to $\gamma \approx 2.6$ but also delay the onset of quantum hyperdiffusion. Finally, a third stage can be identified where the wave packet spreading recovers ballistic diffusion, which is expected because in the end the particle travels in the rest uniform lattice ($V_n = 0$).

To better examine $V_c = 2$ for hyperdiffusion, we show in the inset (a) of Fig. 1 $P_L(t) \equiv \sum_{n=-L}^{+L} |\psi_n(t)|^2$, i.e., the probability for the wave packet to stay in the central sublattice. Consistent with the first-stage ballistic diffusion seen in Fig. 1, $P_L(t)$ in all cases is seen to stay at unity during an initial stage. Later, for $0 \leq V < V_c$, $P_L(t)$ decays appreciably but for $V \geq V_c$, $P_L(t)$ does not decay even for extremely long time scales. This observation hints that quantum hyperdiffusion is connected with the probability leakage from the sublattice to the rest [16]. In addition, cases with larger diffusion exponent γ are seen to have a slower and later decay of $P_L(t)$. The inset (b) of Fig. 1 indicates that the decay of $P_L(t)$ for $1500 < t < 6000$ may be fitted by a nonlinear function $P_L(t) = 1 - \Gamma t^{\alpha}$, with $\alpha = 0.5$ for $V = 1.9$.

To explain the existence of V_c we next consider the band structure of the periodic sublattice and of the rest uniform lattice. For the uniform part, the single-band dispersion relation is $E_u(k) = 2\cos k \in [-2, 2]$, where k is the quasimomentum. By contrast, for the periodic sublattice with $V_n = (-1)^n V$, its dispersion relation is $E_s(k) = \pm\sqrt{V^2 + 4\cos^2 k}$, which yields two energy bands, with $E_s(k) \in [V, \sqrt{V^2 + 4}]$ or $E_s(k) \in [-\sqrt{V^2 + 4}, -V]$. Clearly, then, only if $V < V_c = 2$ can the $E_u(k)$ band partially overlap with the $E_s(k)$ band. In particular, as V approaches V_c and hence the band overlap decreases, the possible ballistic transport velocity distribution on the uniform lattice narrows (this may account for the increase in γ as V increases). If $V > V_c$, an energy band mismatch occurs and then the wave packet launched in the sublattice will be confined by the boundary [19] between the periodic sublattice and the rest.

The above physical picture made the implicit approximation that the periodic sublattice at the center is infinitely long. To lift this approximation we now examine the numerically exact eigenstates of a tight-binding lattice Hamiltonian $H_N = \sum_{n=-N/2+1}^{N/2}(V_n|n\rangle\langle n| - |n+1\rangle\langle n| - |n\rangle\langle n+1|)$, with a total of N sites and V_n defined as before. We denote the N eigenstates by $|\phi^{\alpha}\rangle = \sum_n \phi_n^{\alpha}|n\rangle$, with eigenvalue denoted by E^{α} and ϕ_n^{α} being the amplitude of the αth eigenstate at site n. Three types of $|\phi^{\alpha}\rangle$ are found for $V < V_c$, with their typical behavior shown in Figs. 2(a)–2(c). For type I [Fig. 2(a)], $|\phi_n^{\alpha_{\rm I}}|^2$ is nonzero in $[-L, L]$ but is (essentially) zero outside. For type III [Fig. 2(c)], $|\phi_n^{\alpha_{\rm III}}|^2$ is zero in $[-L, L]$ but is nonzero outside. For type II, $|\phi_n^{\alpha_{\rm II}}|^2$ is appreciably nonzero for all $n \in [-N, N]$. We define $\sigma_{\rm II}^2 = \sum_n n^2 |\sum_{\alpha_{\rm II}} \phi_0^{\alpha_{\rm II}} \phi_n^{\alpha_{\rm II}}(t)|^2$, where $\alpha_{\rm II}$ represent contributions solely by type-II eigenstates. It is seen from Fig. 2(d) that the time dependence of $\sigma_{\rm II}^2$ faithfully captures the quantum hyperdiffusion with $\gamma = 2.4$ [18]. Therefore, quantum coherence among type-II eigenstates is the ultimate origin of quantum hyperdiffusion. One may attempt to use a time-independent scattering theory developed for tight-binding lattice junctions [19] to derive analytical expression for $\sigma_{\rm II}^2$, but this does not help to extract the numerical value of γ because the resulting expression involves a complicated superposition of all type-II eigenstates.

To analyze the eigenstates ϕ^{α} more, we show in Figs. 2(e)–2(g) the von Neumann entropy S^{α} [18,20] vs their eigenenergy E^{α}. Properties of S^{α} suggest that its value should be almost unity for type-III eigenstates and around 0.5–0.6 for type-I eigenstates. As such, points in

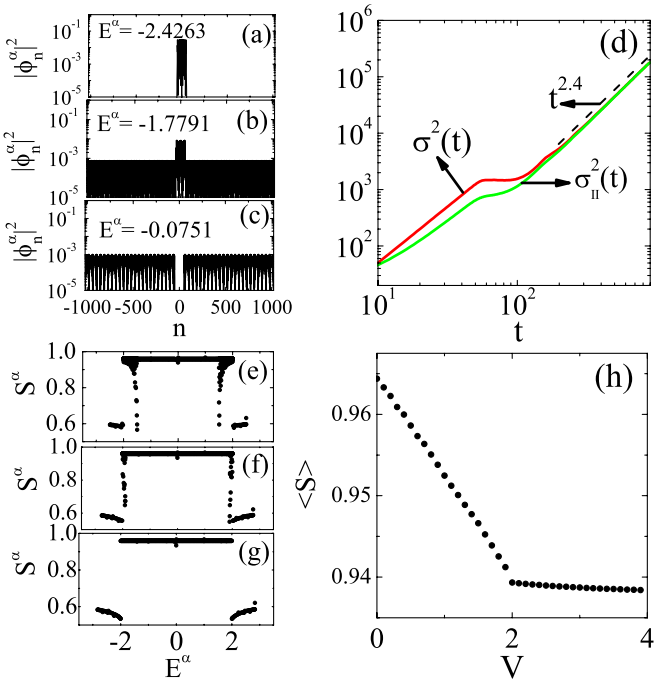

FIG. 2 (color online). Results for a periodic sublattice. $|\phi_n^\alpha|^2$ versus n with $V = 1.5$ for (a) $E^\alpha = -2.4263$, (b) $E^\alpha = -1.7791$, and (c) $E^\alpha = -0.0751$. (d) Time dependency of $\sigma^2(t)$ and $\sigma^2_{\mathrm{II}}(t)$ (defined in the text) for $V = 1.5$. In panels (e)–(g), von Neumann entropy S^α versus eigenenergies E^α is shown, for $V = 1.5$, $V = 1.9$, and $V = 2.0$. (h) Spectrum-averaged von Neumann entropy $\langle S\rangle$ vs V. In all cases, $N = 2048$ and $L = 50$.

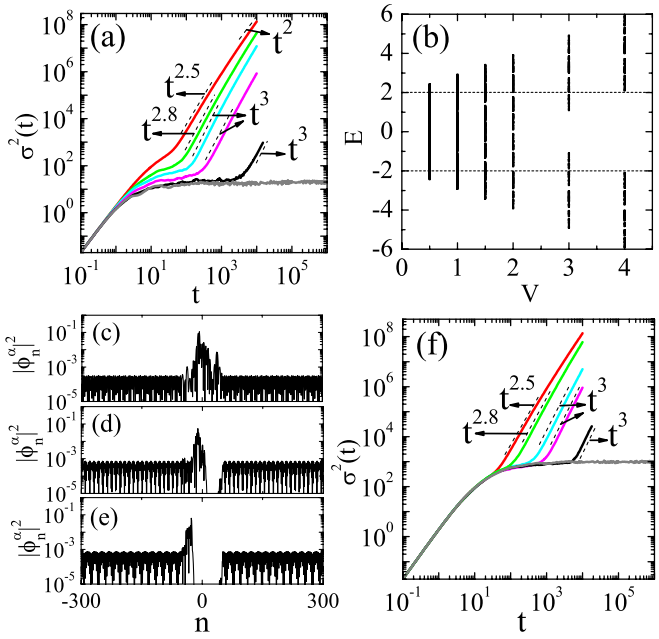

FIG. 3 (color online). (a) Time dependence of $\sigma^2(t)$ for disordered sublattices with $L = 50$, and (from top to bottom) $V = 0.5$, 0.8, 1.0, 1.2, 1.5, and 1.6. (b) Spectra of a long disordered lattice with different values of V. Panels (c)–(e) show three eigenstates of H_N, with $V = 0.5$, $V = 1.0$, and $V = 1.6$. (f) Time dependence of $\sigma^2(t)$ for disordered sublattices, with $V = 0.5$, and a varying length $L = 50$, 100, 200, 250, 500, and 600 (from top to bottom).

Figs. 2(e)–2(g) with $1.0 > S^\alpha > 0.6$ signal the presence of type-II eigenstates. From Figs. 2(e)–2(g), it is seen that E^α of type-II eigenstates always falls in the $E_s(k)$ and $E_u(k)$ bands, thus confirming the above band-structure analysis. Another interesting observation is that as V increases, the number of type-II eigenstates decreases. Indeed, for $V = V_c$ in Fig. 2(g), there does not exist a single type-II eigenstate. The critical value of $V_c = 2$ can also manifest itself clearly even if we average S^α over all eigenstates. Figure 2(h) presents $\langle S\rangle \equiv \frac{1}{N}\sum_\alpha S^\alpha$ vs V, with a clear transition point at $V_c = 2$.

Disordered case.—We now turn to a disordered sublattice; i.e., V_n takes $+V$ or $-V$ randomly, for $n \in [-L, L]$, and $V_n = 0$ otherwise. Parallel results are summarized in Fig. 3 [21]. First of all, the hyperdiffusion exponent γ and the starting time for hyperdiffusion still increases as V increases from a weak value. Interestingly, for $1.0 \leq V \leq 1.5$, the value of γ is saturated at $\gamma \approx 3.0$. For $V \geq V_c \approx 1.6$, quantum hyperdiffusion becomes a rare event: not a single case from our (limited) realizations of the disordered sublattice can yield hyperdiffusion. In Fig. 3(b) we compare the spectra (some analytical results can be found from Ref. [22]) of a long disordered lattice with the $E_u(k)$ band of a uniform lattice (range indicated by dotted lines). Interestingly, even for V well exceeding $V_c \approx 1.6$, there is still significant band overlapping. As such, energy band overlapping does not suffice for hyperdiffusion here. This can be understood from the localization length $\xi \approx 25/V^2$ for states close to the band center of a disordered lattice [23]. For $V = 1.6$, $\xi \approx 9.8 < L/5$, it then becomes highly rare for a state launched from the center of a disordered sublattice to have appreciable probability to travel to the boundary at $n = \pm L$. On the other hand, the localization becomes irrelevant when ξ becomes comparable to the size of the disordered sublattice. In these cases the mechanism for hyperdiffusion is expected to be similar to the periodic case. Indeed, the typical type-II eigenstate of H_N (now with a disordered lattice embedded in the center) for $N = 2048$ and $V = 0.5$ shown in Fig. 3(c) is similar to the periodic case [see Fig. 2(b)]. As V increases from $V = 0.5$, there are less type-II eigenstates that can contribute to hyperdiffusion. Figures 3(d) and 3(e) show the fate of type-II eigenstates when V further increases: they simply become more localized in $[-L, L]$ and eventually, as we reach the regime of $\xi/L < 1/5$ [Fig. 3(e)], all of them (investigated in our 30 realizations) lose their overlap with the initial state localized at $n = 0$ [24]. To confirm that our analysis here is scale invariant, we next fix $V = 0.5$ (hence $\xi = 100$) but vary L, with the diffusion results shown in Fig. 3(f). Once again we find that γ increases with

decreasing ξ/L in the regime of $\xi/L > 1/2$. For $200 \leq L \leq 500$ (i.e., $1/5 < \xi/L < 1/2$), γ is saturated at $\gamma \approx 3.0$. The numerical finding in this regime also agrees with Ref. [16]. For $L = 600$ ($\xi/L < 1/5$), hyperdiffusion disappears for all the disorder realizations we investigated, in agreement with Fig. 3(a) [24].

Quasiperiodic case.—Finally, we carry out a parallel study for quasiperiodic sublattices, which turn out to be most interesting. Quasiperiodic systems are between periodic and disordered systems and possess intriguing energy spectra and eigenstate structure [25]. Here we take a Fibonacci sublattice as an example, where V_n takes $+V$ or $-V$ according to a Fibonacci sequence [25] for $n \in [-L, L]$. It is well known that a Fibonacci lattice yields singular continuous energy spectra and critical eigenstates (that are neither localized nor extended). As seen from Fig. 4, for fixed L the hyperdiffusion exponent γ may be also tuned by changing V [26]. Surprisingly, as V reaches $V = 2.0$, we find $\gamma \approx 3.4 > 3.0$. This diffusion exponent is considerably larger than that found in Ref. [16] for disordered cases. For $2.0 < V < 2.9$, γ changes little, indicating that such a large diffusion exponent can be robust. As we increase V further, a clear transition occurs for $V = V_c \approx 3.0$, beyond which hyperdiffusion can no longer be observed. Because eigenstates of a quasiperiodic lattice are not localized in general, it is safe to use a band-mismatch picture to account for $V_c \approx 3.0$. To that end, in inset (a) of Fig. 4 we compare the energy spectra of a long Fibonacci lattice with the $E_u(k)$ band (the range is indicated by dotted lines). Because of the fractal nature of the spectra of a Fibonacci lattice, many subbands can be seen. As V increases, the number of subbands overlapping with the $E_u(k)$ band decreases. In the regime of $2.0 < V < 2.5$, there is only one cluster of subbands inside the $E_u(k)$ band. This cluster of subbands then gradually shifts outside the $E_u(k)$ band as V further increases. For $V \geq 3.0$, all the subbands of the Fibonacci lattice have moved outside the $E_u(k)$ band; i.e., the band of the sublattice and that of the uniform lattice totally mismatch. This finally explains why hyperdiffusion is lost for $V \geq 3.0$.

It is then important to investigate if the hyperdiffusion exponent can be tuned to go beyond $\gamma \approx 3.4$. We hence perform extensive numerical studies by also varying the size of the sublattice. Cases with $\gamma > 4$ are observed. In particular, we obtain that if $L \geq 200$, then we obtain the largest exponent $\gamma \approx 4.7$ (see Fig. 4 for the $t^{4.7}$ fitting and the Supplemental Material for individual realizations), with the critical value of V still at $V_c \approx 3.0$. Thus, in the quasiperiodic case here, there is one additional tuning parameter to control the hyperdiffusion exponent. Because the self-similar structure of the sublattice spectra and of the associated eigenstates can persist to a finer scale as L increases, the L dependence of γ is a unique feature connected with the fractal nature of a quasiperiodic sublattice.

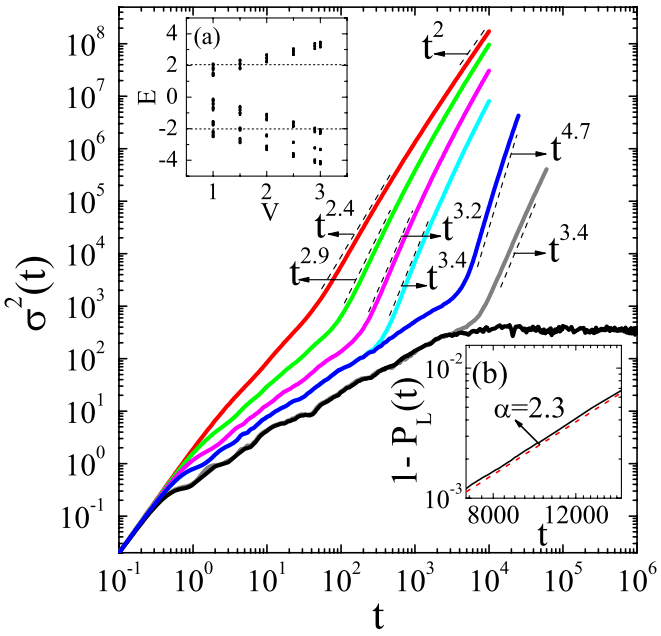

FIG. 4 (color online). The case with $\sigma^2(t) \sim t^{4.7}$ fitting represents time dependence of $\sigma^2(t)$ for a Fibonacci sublattice with $L = 200$ and $V = 2.0$. Others are for $L = 50$ and (from top to bottom) $V = 0.5$, 1.0, 1.5, 2.0, 2.9, and 3.0. Inset (a) shows the spectra of a long Fibonacci lattice with different values of V. In the case of $V = 2.0$ and $L = 200$ and for $7000 < t < 15\,000$, inset (b) shows (double-logarithmic scale) a nonlinear fitting of $P_L(t)$ using $P_L(t) = 1 - \Gamma t^{\alpha}$, with $\alpha = 2.3$.

Discussion.—Finally, we discuss a phenomenological and semiquantitative explanation of the hyperdiffusion exponents, by making use of the nonlinear fitting $P_L(t) = 1 - \Gamma t^{\alpha}$, already shown in the insets of Figs. 1 and 4. During the time window for which the nonlinear fitting works well, the probability for the wave packet being on the rest uniform lattice increases nonlinearly. Assuming that the velocity of the ballistic transport on the rest uniform lattice is sharply peaked at v, one then obtains $\sigma^2(t) \sim \sum_{n=0}^{+\infty} n^2 \int_0^t dt' (-\frac{dP_L(t')}{dt'}) \delta[n - (t - t')v - L]$, which leads to $\sigma^2(t) \sim t^{\alpha+2}$ if all other t polynomials with orders of $\alpha + 1$ or below are neglected [18]. This then predicts a hyperdiffusion behavior with $\gamma \approx \alpha + 2$. For the two examples shown in the insets of Figs. 1 and 4, the analysis here gives $\gamma \approx 2.5$ and $\gamma \approx 4.3$, which is reasonably close to our numerical observations of $\gamma \approx 2.6$ and $\gamma \approx 4.7$. The interpretation given in Ref. [16] using a linear behavior of $P_L(t)$ can hence be extended to the nonlinear regime.

In conclusion, the quantum hyperdiffusion displayed by wave packet spreading from a sublattice to a uniform lattice is a typical feature and can be analyzed in a rather unified fashion. Interestingly, the quasiperiodic cases are found to generate the largest hyperdiffusion exponents (with $\gamma > 3$). Observations and analysis presented here should stimulate experimental studies and even a formal theory of quantum hyperdiffusion.

This work was supported by the National Natural Science Foundation of China (Grants No. 10974097 and No. 11175087), and by National Key Projects for Basic Research of China (Grant No. 2009CB929501). J. G. is supported by Academic Research Fund Tier I, Ministry of Education, Singapore (Grant No. R-144-000-276-112). B. L. is supported by a startup fund from Tongji University.

*Corresponding author.
pqtong@njnu.edu.cn

[1] J. P. Bouchaud and A. Georges, Phys. Rep. **195**, 127 (1990).
[2] B. I. Henry, T. A. M. Langlands, and P. Straka, in *Complex Physical, Biophysical and Econophysical Systems*, World Scientific Lecture Notes in Complex Systems, edited by R. L. Dewar and F. Detering (World Scientific, Singapore, 2010), Vol. 9.
[3] B. D. Hughes, *Random Walks and Random Environments* (Clarendon Press, Oxford, 1995).
[4] R. Metzler and J. Klafter, Phys. Rep. **339**, 1 (2000).
[5] P. Hänggi, P. Talkner, and M. Borcovec, Rev. Mod. Phys. **62**, 251 (1990).
[6] Y. He, S. Burov, R. Metzler, and E. Barkai, Phys. Rev. Lett. **101**, 058101 (2008).
[7] K. Lü and J.-D. Bao, Phys. Rev. E **76**, 061119 (2007).
[8] P. Siegle, I. Goychuk, P. Talkner, and P. Hänggi, Phys. Rev. E **81**, 011136 (2010); P. Siegle, I. Goychuk, and P. Hänggi, Phys. Rev. Lett. **105**, 100602 (2010); P. Siegle, I. Goychuk, and P. Hänggi, Europhys. Lett. **93**, 20002 (2011).
[9] D. E. Katsanos, S. N. Evangelou, and S. J. Xiong, Phys. Rev. B **51**, 895 (1995).
[10] P. W. Anderson, Phys. Rev. **109**, 1492 (1958).
[11] T. Geisel, R. Ketzmerick, and G. Petschel, Phys. Rev. Lett. **66**, 1651 (1991).
[12] S. Abe and H. Hiramoto, Phys. Rev. A **36**, 5349 (1987); H. Hiramoto and S. Abe, J. Phys. Soc. Jpn. **57**, 230 (1988); **57**, 1365 (1988).
[13] F. Piéchon, Phys. Rev. Lett. **76**, 4372 (1996).
[14] R. Ketzmerick, K. Kruse, S. Kraut, and T. Geisel, Phys. Rev. Lett. **79**, 1959 (1997).
[15] P. Q. Tong, B. W. Li, and B. B. Hu, Phys. Rev. Lett. **88**, 046804 (2002).
[16] L. Hufnagel, R. Ketzmerick, T. Kottos, and T. Geisel, Phys. Rev. E **64**, 012301 (2001).
[17] For example, J. Billy *et al.*, Nature (London) **453**, 891 (2008); G. Roati *et al.*, Nature (London) **453**, 895 (2008).
[18] See Supplemental Material at http://link.aps.org/supplemental/10.1103/PhysRevLett.108.070603 for some computational details and a more detailed discussion of the relationship between $P_L(t)$ and hyperdiffusion exponents.
[19] J. B. Gong, D. Poletti, and P. Hänggi, Phys. Rev. A **75**, 033602 (2007).
[20] L. Y. Gong and P. Q. Tong, Phys. Rev. E **74**, 056103 (2006).
[21] The results for the disordered case are obtained after averaging over 30 realizations of the disordered sublattice. Also see our Supplemental Material [18] for individual realizations.
[22] D. J. Thouless, J. Phys. C **3**, 1559 (1970).
[23] B. Kramer and A. MacKinnon, Rep. Prog. Phys. **56**, 1469 (1993).
[24] The observed disappearance of the hyperdiffusion is based on the fixed 30 realizations of the disordered sublattice we investigated, indicating that the hyperdiffusion behavior becomes highly rare: they can be found again if many more realizations are investigated.
[25] M. Kohmoto, L. P. Kadanoff, and C. Tang, Phys. Rev. Lett. **50**, 1870 (1983); G. Gumbs and M. K. Ali, Phys. Rev. Lett. **60**, 1081 (1988); M. Dulea, M. Severin, and R. Riklund, Phys. Rev. B **42**, 3680 (1990); G. Y. Oh and M. H. Lee, Phys. Rev. B **48**, 12 465 (1993).
[26] Results presented in Fig. 4 are averaged over 30 different realizations of V_n drawn from a long Fibonacci series. See our Supplemental Material [18] for more details.